

Some Aspects of Electric Power Equipment Modelling through Sustainability Key Concepts

CORNELIA A. BULUCEA¹ DORU A. NICOLA¹ MARC A. ROSEN²
NIKOS E. MASTORAKIS³ CARMEN A. BULUCEA⁴

¹Faculty of Electrical Engineering, University of Craiova
ROMANIA

²Faculty of Engineering and Applied Science, University of Ontario Institute of Technology
CANADA

³Military Institutes of University Education, Hellenic Naval Academy
GREECE

⁴Faculty of Medicine, University of Medicine and Pharmacy of Craiova
ROMANIA

Emails: abulucea@em.ucv.ro, dnicola@em.ucv.ro, marc.rosen@uoit.ca, mastor@hna.gr,
carmen.bulucea@umfcv.ro

Abstract: Enhancements are made to the concept that technical systems and processes involving energy conversion, and particularly electric power equipment, need to be linked to environment engineering, since the concept of sustainable development should emphasize two complementary aspects. The first is related to the design of electrical equipment in order to achieve high energy efficiency during all life stages of a system, and the second takes into consideration the environmental impact of technical systems operation, since biological ecosystems generally are not free of anthropogenic influences. These are the reasons that, over the last few decades, international legislation has required environmental impact assessment to be carried out for all phases of the life electrical equipment, according to Life Cycle Assessment, which includes the production, use and end-of-life phases. Following the notion that Nature demonstrates sustainable energy conversion, this work focuses on highlighting that industrial ecology permits an alternate view of anthropogenic applications, related both to technical and environmental reference systems. The study addresses some aspects, using energy conversion processes during the operation of power transformers and induction motors as modeling examples of sustainable electric equipment. Based on the model equations, this article presents the structural diagrams method, as a modeling method for a three-phase electric transformer and induction motor in dynamic regimes, according to an ecosystem pattern. The overall objective is to enhance understanding of how anthropogenic activities can be viewed in concert with the entire system on Earth.

Key-Words: Electric power equipment, electromagnetic torque, exergy, induction motor, power transformer, structural diagram, sustainability dynamics

1 Introduction

Electrical power is used all over the world, and standards of life and development of civilization are often interpreted in correlation with the use of electricity [1-6]. Nonetheless, concerns and questions have been raised regarding, how to achieve a sustainable industrial metabolism. Integrating technical and ecological aspects represents a significant challenge to humanity within the present industrial world. In line with this idea, sustainability concepts can help improve understanding of the

efficiencies of electric power equipment and systems and guide improvement efforts [1-14].

Traditionally, the basic concepts of energy, exergy and embodied energy are founded in the fields of physics and engineering, although they have environmental and economical significance as well.

These concepts can be explained, interpreted and applied in a more universal manner, due to their multidisciplinary traits [1-3,13-16].

Taking a holistic view, this study focuses on highlighting that industrial ecology permits an alternate view of anthropogenic applications, related

both to technical and environmental reference systems.

In line with this idea, in order to enhance thinking that anthropogenic activities can and should be viewed in concert with the entire system on Earth, this study addresses some aspects, considering energy conversion processes during the operation of power transformers and induction motors, by modelling an electric power transformer in the life use phase, and an induction motor operating within an electrically driven system according to an industrial ecosystem pattern. Based on the model equations, the article presents the structural diagram method, as a modeling method for a three-phase electric transformer and induction motor in dynamic regimes, within the framework of industrial ecology.

2 Power Transformer Modelling through Structural Diagram Method

Three-phase transformers are widely used since three phase power is the widespread way to produce, transmit and use electrical energy [1-2,16-20]. A three-phase transformer transfers electric power from the three-phase primary winding through an inductively coupled three-phase secondary winding, changing values of three-phase RMS voltage and current. Most commonly, the transformers windings are wound around a ferromagnetic core [1,20].

Over the last few decades, international legislation have required environmental impact assessment be carried out for all phases of transformer life [1,16-20], according to Life Cycle Assessment tool, which includes the production phase, use phase and end-of-life phase. Modelling of all these transformer life stages might offer solutions for further improvement potential, focusing on technologies that reduce the electricity losses during the use phase, and on alternative materials for reducing human health and environmental impacts [1, 16-20].

The operation principle of a three phase transformer follows. Varying currents flowing in the primary winding (due to the varying phase voltages u_A , u_B and u_C) create a varying magnetic flux in the transformer core, and thus a varying magnetic field through the secondary winding [1,18]. This varying magnetic field induces a varying electromotive force in the secondary winding. If a three-phase electric load is connected to the secondary winding, electrical energy is transferred from the primary circuit through the transformer to the load. Since u_a , u_b and u_c are the secondary phase voltage, the load three-phase currents system i_a , i_b and i_c will be at the same time the transformer secondary winding currents system. Note that these currents represent the feedback (or inverse reaction) between the electric load and the power transformer. In line with this idea, the three-phase transformer representation as an industrial ecosystem is depicted in Fig. 1.

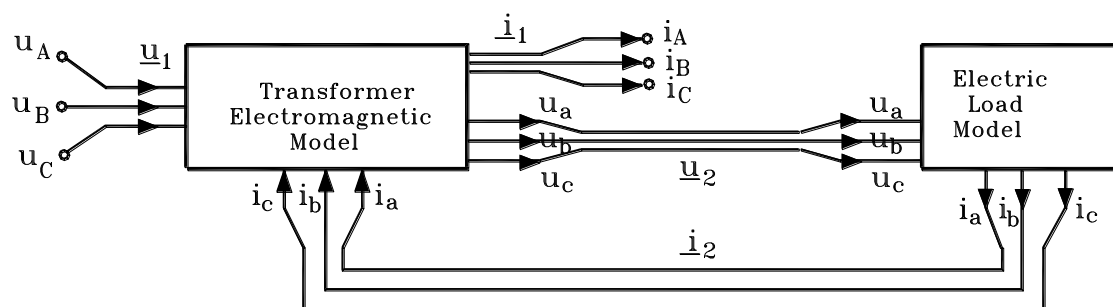


Fig. 1 Three-phase transformer representation

Since efficiency standards can be expressed in terms of electrical efficiency depending on load characteristics, in an attempt to improve the power transformer efficiency, the structural diagram method is presented below for analyzing the three-phase transformer operation in the life use phase.

The classic models, meaning the equivalent electric schemes and the phasor diagrams of power transformer, could be considered only in a

permanent regime operation, when all the state quantities have a sinusoidal variation in time. In dynamic regimes, they lose their validity and other models should be developed [1,18].

As a principle, with electrical transformer modelling one can understand the use of conventional representations (geometric constructions, electrical circuits, structural diagrams etc.) to describe the behavior (or for the simulation)

of various operation states or regimes [2,14].

Physically, dynamic regimes of electric transformers are characterized by the variation in time of “electromagnetic status”, meaning the currents and fluxes. Qualitatively, the dynamic phenomena of an electromagnetic nature in the electric transformers are fast and develop with small time-constants (usually, between 1 and 100 ms).

In this study the three-phase electromagnetic phenomena will be described into the space phasors theory, taking into consideration the relations [18]:

$$\begin{aligned} \underline{u}_1 &= \frac{2}{3} \cdot (u_A + a \cdot u_B + a^2 \cdot u_C) \\ \underline{i}_1 &= \frac{2}{3} \cdot (i_A + a \cdot i_B + a^2 \cdot i_C) \\ \underline{u}_2 &= \frac{2}{3} \cdot (u_a + a \cdot u_b + a^2 \cdot u_c) \\ \underline{i}_2 &= \frac{2}{3} \cdot (i_a + a \cdot i_b + a^2 \cdot i_c) \end{aligned} \tag{1}$$

With space phasors the modeling representation of the three-phase transformer becomes identical with that of the single phase transformer [18-19]. The distinction between them is of pure mathematical nature, emphasizing that in case of three-phase transformer all variables, including the external ones (\underline{u}_1 = primary voltage; \underline{i}_1 = primary current; \underline{u}_2 = secondary voltage and \underline{i}_2 = secondary current), as well as the internal ones are not real but complex mathematical quantities. In this context, in the study of the three-phase transformer one can use the space phasors equations, and the structural diagrams will encompass the complex quantities.

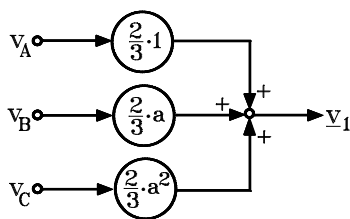


Fig.2 Pattern of space phasor \underline{v}_1 built with phase quantities v_A, v_B, v_C

According to space phasors relations (1) and taking into consideration the relations for three-phase system reconstituting, in Fig.2 and Fig.3, respectively had been represented two generic patterns (as a form of structural diagram) of the variables transformation. These models are corresponding, respectively, to the phase quantities triplet v_A, v_B, v_C which built the space phasor \underline{v}_1 (direct transformation in fixed coordinates) and to the rebuild of the phase variables v_A, v_B, v_C

(reverse transformation in fixed coordinates), according to the following relations:

$$\begin{aligned} v_A &= \text{Re}\{\underline{v}_1\} + v_0 \\ v_B &= \text{Re}\{a^{-1} \cdot \underline{v}_1\} + v_0 \\ v_C &= \text{Re}\{a^{-2} \cdot \underline{v}_1\} + v_0 \end{aligned} \tag{2}$$

where $v_0 = \frac{1}{3} \cdot (v_A + v_B + v_C)$ represents the zero sequence component of the three-phase system, and $\text{Re}\{\}$ denotes the real part of the complex quantity (between braces).

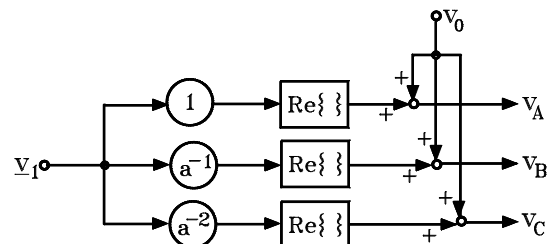


Fig.3 Pattern of phase quantities v_A, v_B, v_C rebuild from space phasor \underline{v}_1

Mathematically, the processes dynamics of electric transformers are described by differential equations which, in most cases, are nonlinear. Based on the mathematical model equations, we present the structural diagrams method in this study, as a modeling method of electric transformers for the life use phase in dynamic regimes. One benefit of this approach is derived from the easy conversion of structural diagrams in Matlab-Simulink implementations [1-2,18-19].

Basically, a structural diagram [1,18] represents the graphical image of the differential equations corresponding to the mathematical model of the dynamic regime of the physical system taken into account. Hence, real or complex variables are represented by lines with arrows and graphical symbols are associated with the mathematical operations effected on the variables. In this context, a number of “arrangements” are described in which mathematical equations (equations of voltages and fluxes) of the three-phase electric transformer can be represented directly by structural diagrams. Since in the structural diagrams, the variables are always represented by lines with arrows, the load current \underline{i}_2 (which are flowing through the secondary winding) represent the feedback reaction between the power transformer and the electric load (connected at the secondary winding terminals).

For a three-phase transformer, electrically and magnetically symmetric, one could obtain the equations corresponding to the mathematical pattern, written with phase quantities space phasors in fixed coordinates, according to the following system:

$$\begin{aligned}
 \underline{u}_1 &= R_1 \cdot \underline{i}_1 + \frac{d\underline{\psi}_1}{dt} \\
 -\underline{u}'_2 &= R'_2 \cdot \underline{i}'_2 + \frac{d\underline{\psi}'_2}{dt} \\
 \underline{\psi}_1 &= L_{\sigma 1} \cdot \underline{i}_1 + \underline{\psi}_{u1} \\
 \underline{\psi}'_2 &= L'_{\sigma 2} \cdot \underline{i}'_2 + \underline{\psi}_{u1} \\
 \underline{i}_1 + \underline{i}'_2 &= \underline{i}_{1\mu} \\
 \underline{i}'_2 &= \frac{w_2}{w_1} \cdot \underline{i}_2 \\
 \underline{u}_2 &= (-\underline{u}'_2) \cdot \left(-\frac{w_2}{w_1}\right)
 \end{aligned} \tag{3}$$

where \underline{u}_1 = primary voltage; \underline{i}_1 = primary current; \underline{u}_2 = secondary voltage; \underline{i}_2 = secondary current; $\underline{\psi}_1$ = primary magnetic flux; $\underline{\psi}_2$ = secondary magnetic flux; $\underline{\psi}_{u1}$ = main (useful) magnetic flux; $\underline{i}_{1\mu}$ = magnetizing current; R_1 = primary phase resistance; R_2 = secondary phase resistance; $L_{1\sigma}$ = primary leakage inductance; and $L_{2\sigma}$ = secondary leakage inductance.

In order to be used for the structural diagrams building, the equations in (3) are written as follows:

$$\begin{aligned}
 \underline{\psi}_1 &= \int_0^t (\underline{u}_1 - R_1 \cdot \underline{i}_1) \cdot dt + \underline{\psi}_1(0) \\
 \underline{i}'_2 &= \frac{w_2}{w_1} \cdot \underline{i}_2 \\
 \underline{i}_1 &= \frac{\underline{\psi}_1 - \underline{\psi}_{u1}}{L_{\sigma 1}} \\
 \underline{i}_1 + \underline{i}'_2 &= \underline{i}_{1\mu} \\
 \underline{\psi}'_2 &= \underline{\psi}_{u1} + L'_{\sigma 2} \cdot \underline{i}'_2 \\
 -\underline{u}'_2 &= R'_2 \cdot \underline{i}'_2 + \frac{d\underline{\psi}'_2}{dt} \\
 \underline{u}_2 &= (-\underline{u}'_2) \cdot \left(-\frac{w_2}{w_1}\right)
 \end{aligned} \tag{4}$$

Note that system (4) needs to be completed with the magnetization curve $\phi_u = f(i_{1\mu})$ of the transformer ferromagnetic core. The magnetization characteristic of any magnetic circuit made by ferromagnetic material contains information about the main flux saturation degree. Even under the assumption of negligible magnetic hysteresis

phenomenon, when the space phasors $\underline{\psi}_{u1}$ and $\underline{i}_{1\mu}$ have a sin phase variation, one can develop two patterns: linear and non-linear.

One can obtain a linear model under the assumption that the ferromagnetic core magnetization characteristic $\phi_u = f(i_{1\mu})$ can be approximated by a straight line. Hence, for the case of a linear model, the transformer ferromagnetic core is considered as non-saturated, and one can apply the principle of effects super-position, taking into consideration the main cyclical inductance of the transformer primary. Consequently, the structural diagram of linear electromagnetic pattern of three-phase transformer is depicted as in Fig. 4.

The three-phase transformer non-linear model takes into consideration the non-linear dependence between the main fascicular magnetic flux and the magnetizing current. On a broader front, the magnetizing characteristic of the transformer ferromagnetic core has a non-linear trait. Actually, the magnetizing curve $\phi_u = f(i_{1\mu})$ is obtained by testing points and in the literature one can find it in tabular form.

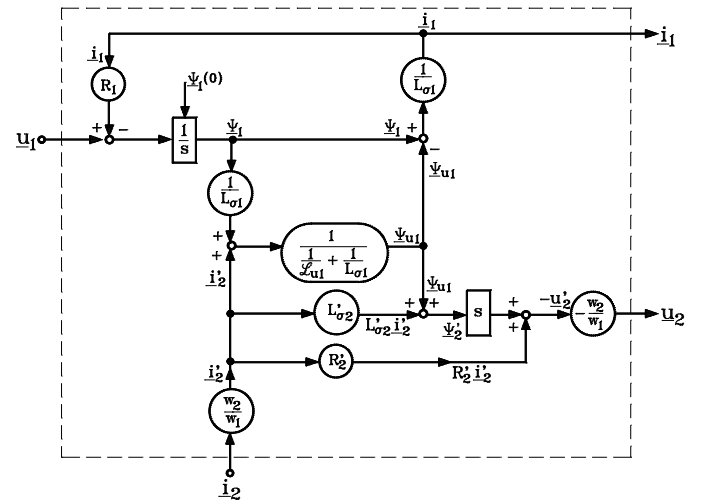


Fig. 4 Structural diagram with space phasors of three-phase transformer linear model

For each value of the useful fascicular flux ϕ_u , the main magnetic flux ψ_{u1} (through the surface delimited by all turns w_1 of primary phase winding) is given by $\psi_{u1} = w_1 \cdot \phi_u$. Moreover, neglecting the losses in the transformer ferromagnetic core, the total useful flux space phasor $\underline{\psi}_{u1}$ and the magnetizing current space phasor $\underline{i}_{1\mu} = \underline{i}_1 + \underline{i}'_2$ are collinear. So they can be mathematically translated

by the following relation:

$$\frac{\psi_{u1}}{|\psi_{u1}|} = \frac{i_{1\mu}}{|i_{1\mu}|} \Rightarrow \psi_{u1} = |\psi_{u1}| \cdot \frac{i_{1\mu}}{|i_{1\mu}|} \quad (5)$$

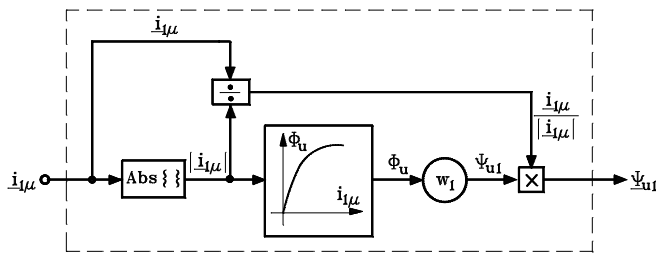


Fig. 5 Structural diagram with space phasors of magnetization circuit

Consequently, if the calculation block of the absolute value of a complex quantity it is noted by “Abs { }”, then for the non-linear magnetization branch-circuit (with $i_{1\mu}$ = incoming quantity and ψ_{u1} = outgoing quantity) one could conceive and represent a structural subsystem, exactly as in Fig. 5.

Further, for the non-linear pattern of the three-phase transformer one could represent the structural diagram with the variables represented by the space phasors, as in Fig. 6, where the magnetization circuit structural subsystem is represented as the “Figure” rectangle.

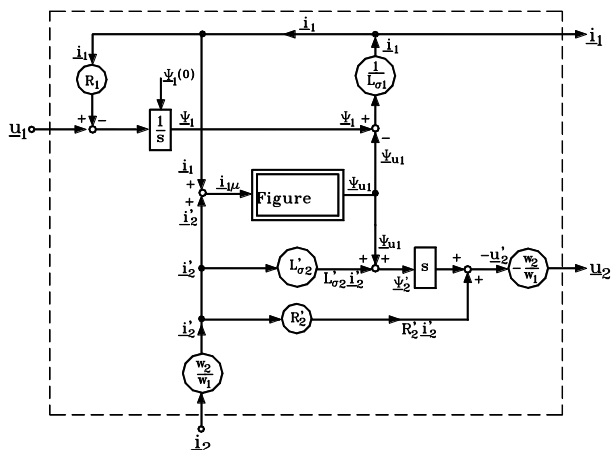


Fig. 6 Structural diagram with space phasors of three-phase transformer non-linear model

In order to highlight the interactions and feedback loops of this industrial ecosystem, representations corresponding to the space phasors \underline{u}_1 , \underline{i}_1 , \underline{u}_2 and \underline{i}_2 , respectively, in all structural diagrams built for the three-phase transformers. Obviously, the representations are made with space phasors of the phase quantities. Since this is a common feature of all modelling diagrams of three-phase transformers, one should emphasize that structural diagrams are

beginning with input variables and ending with output variables of complex quantity type.

3 Modelling of Electromagnetic Torque Developed by Induction Motor

Within the framework of industrial ecology, the exergy concept, which is a measure of energy quality, can be used to enhance understanding and help improve the efficiencies of electric power equipment which convert energy [1-5,7,13-16,22].

In physics and engineering, work is a specific form of action, and exergy is defined based on work, i.e. ordered motion, or ability to perform work [1-5,7,13-16,22]. While energy is a measure of quantity only, exergy is a measure of quantity and quality or usefulness.

Since exergy is a measure of the potential of a system to do work, the electromagnetic torque M developed by an induction motor can be interpreted as the driving force of useful work, i.e. the electric motor output exergy [1-5,7,13-16,22].

Utilization of an induction motor with a rotor squirrel cage in electrically driven systems became possible solely in the conditions of a three-phase supply system with controlled variable frequency and r.m.s. voltages or currents, namely a machine-side converter [21-27]. This research extends earlier work by the authors [1-5,7,21-22].

3.1 Induction Motor Operating at Variable Frequency and Controlled Flux

Starting from the observation that an industrial ecosystem does not have a single equilibrium point, but rather the system moves among multiple stable states [7-13], we approach the sustainable operation at different speeds of an induction motor within the framework of industrial ecology. In line with this idea, the dynamic regimes in induction motor operation can be viewed as representing the industrial ecosystem movement among points of equilibrium [3-5].

Induction motor speed regulation is determined by examining the machine-side converter (that ensures the supply at variable voltage and variable frequency (VVVF)) and the electric machine as an assembly. The induction motor speed variation is based on stator voltage and frequency variation, so to achieve high energy and exergy efficiencies, the first requirement of system control concerns passing of the motor operation equilibrium point from one stable state to another. Based on the mechanical characteristics $M=f(n)$ of the induction motor

operation at variable speed [3-5] we highlight an analogy between this electrical power system and an ecosystem: appropriate technical system control must be achieved for reducing exergy destruction when the equilibrium point passes from one stable state (represented by the operation point on a certain mechanical characteristic) to another stable state (with the operation point on another mechanical characteristic). This observation implies the system control needs to be assessed next, taking into consideration the induction motor operating at controlled flux and the machine-side converter (that ensures the supply at variable voltage and variable frequency) as a whole.

The operation at variable frequency with controlled flux is preceded for induction motors in drive systems with vectorial control [1,7,21-27]. The vectorial regulation and control method is based on space phasor theory, taking into consideration the control of both the flux and the induction machine electromagnetic torque M . In principle, the stator current space phasor is decomposed into two perpendicular components (a flux component and a torque component) which are separately controlled. One could analyze the permanent harmonics regime of variable frequency operation with controlled stator flux, controlled useful flux or controlled rotor flux. As an example, we present the operation with controlled stator flux [1,21].

The following relations can be derived for the stator current components [21]:

$$I_{sx} = \frac{\psi_s}{L_s} + \frac{1-\sigma}{\sigma L_s} \frac{\psi_s}{\frac{R_r'}{\omega_r \sigma L_r'} + \frac{\omega_r \sigma L_r'}{R_r'}} \frac{\omega_r \sigma L_r'}{R_r'} \quad (6)$$

$$I_{sy} = \frac{1-\sigma}{\sigma L_s} \frac{\psi_s}{\frac{R_r'}{\omega_r \sigma L_r'} + \frac{\omega_r \sigma L_r'}{R_r'}}$$

The absolute value of the stator current can be determined with the formula $I_s = (I_{sx}^2 + I_{sy}^2)^{1/2}$.

Within an ecological framework, the electromagnetic torque M is related to the system output exergy. We can express M in complex coordinates axes system (oriented on $\underline{\psi}_s$) as

$$\begin{aligned} M &= 3p \cdot \text{Im}\{ \underline{I}_s \cdot \underline{\psi}_s^* \} \\ &= 3p \cdot \text{Im}\{ (I_{sx} + jI_{sy}) \cdot \psi_s \} \\ &= 3p \cdot \psi_s \cdot I_{sy} \end{aligned} \quad (7)$$

Substituting I_{sy} from (6), the torque relation becomes

$$M = 3p \cdot \frac{1-\sigma}{\sigma L_s} \cdot \frac{\psi_s^2}{\frac{R_r'}{\omega_r \sigma L_r'} + \frac{\omega_r \sigma L_r'}{R_r'}} \quad (8)$$

If the stator flux ψ_s is constant, the

electromagnetic torque magnitude depends on the rotor current pulsation ω_r but not the stator supply frequency f_s . The torque curve $M=f(\omega_r)$ at $\psi_s=\text{const.}$ is not linearly dependent on ω_r , having two symmetrical extremes:

$$\frac{\partial M}{\partial \omega_r} = 0; \quad \omega_{rk\psi_s} = \pm \frac{R_r'}{\sigma \cdot L_r'}; \quad (9)$$

$$M_{k\psi_s} = M(\omega_{rk\psi_s}) = \pm \frac{3p}{2} \cdot \frac{1-\sigma}{\sigma \cdot L_s} \cdot \psi_s^2$$

The dependence of $M=f(\omega_r)$ at $\psi_s=\text{const.}$ is shown in Fig. 7.

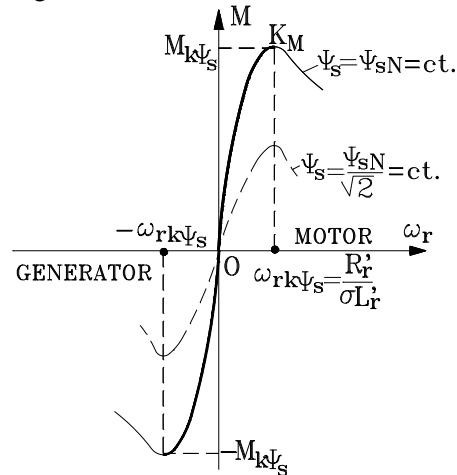


Fig. 7 Torque characteristic $M=f(\omega_r)$ at controlled stator flux

In a steady-state regime, a system stable operation (with $\partial M/\partial \omega_r > 0$) is performed only on the ascendant zone of the characteristic $M=f(\omega_r)$ in Fig. 5 and corresponds at small rotor pulsations to the condition $|\omega_r| \leq \omega_{rk\psi_s}$. The mechanical characteristics family $M=f(n)$ of the induction motor operating at $\psi_s=\text{const.}$, for different stator frequencies f_s , are shown in Fig. 8.

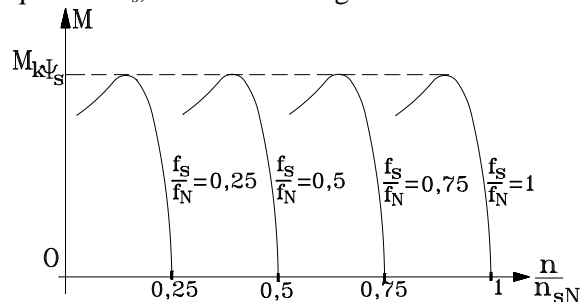


Fig. 8 Mechanical characteristics $M=f(n)$ at $\psi_s=\text{const.}$ for different frequency f_s values ($f_s \leq f_N$)

The constant stator flux magnitude ψ_s for any stator frequency f_s and torque M (respectively, any rotor pulsation ω_r) imposes an exact control of either the supply voltage U_s or the supply current I_s . We

Based on the curves of Fig. 10 and the mentioned relations the constant flux levels are determined:

$$\psi_s = \psi_{sN} = ct. \quad (15)$$

$$\psi_u = f_1\left(\pm \frac{R'_r}{L_{r\sigma}}\right) = \psi_s \cdot \frac{L_u}{L_s} \cdot \frac{\sqrt{2}}{\sqrt{1 + \left(\frac{\sigma L'_r}{L_{r\sigma}}\right)^2}} = ct.$$

$$\psi'_r = f_2\left(\pm \frac{R'_r}{L_{r\sigma}}\right) = \psi_s \cdot \frac{L_u}{L_s} \cdot \frac{1}{\sqrt{1 + \left(\frac{\sigma L'_r}{L_{r\sigma}}\right)^2}} = ct. \quad \left(\psi'_r = \frac{\psi_u}{\sqrt{2}}\right)$$

For these constant values of fluxes Ψ_s , Ψ_u and Ψ'_r , an exergetic analysis imposes the electromagnetic torque characteristics $M = f(\omega_r)$ and stator current characteristics $I_s = f(\omega_r)$ are compared on the stable operation intervals.

3.1.1 Electromagnetic Torques Comparison at $\Psi_s = ct.$, $\Psi_u = ct.$ and $\Psi'_r = ct.$

For the three subsequent cases, the electromagnetic torque M has the following expressions:

a) When stator flux is constant $\Psi_s = ct.$:

$$M = \frac{2 \cdot M_{k\psi_s}}{\frac{\sigma \cdot L'_r \cdot \omega_r}{R'_r} + \frac{R'_r}{\sigma \cdot L'_r \cdot \omega_r}} \quad (16)$$

$$M_{k\psi_s} = \frac{3p}{2} \cdot \frac{1 - \sigma}{\sigma \cdot L_s} \cdot \psi_s^2$$

b) When useful flux is constant $\Psi_u = ct.$:

$$M = \frac{2 \cdot M_{k\psi_u}}{\frac{L'_{r\sigma} \cdot \omega_r}{R'_r} + \frac{R'_r}{L'_{r\sigma} \cdot \omega_r}} \quad (17)$$

$$M_{k\psi_u} = \frac{3p}{2} \cdot \frac{1}{L'_{r\sigma}} \cdot \psi_u^2$$

c) When rotor flux is constant $\Psi'_r = ct.$:

$$M = 3p \cdot \frac{\omega_r}{R'_r} \cdot \psi'^2_r \quad (18)$$

Moreover, according to the constant flux levels (15), between the maximum torques $M_{k\psi_s}$ and $M_{k\psi_u}$ the following recurrence relationship can be demonstrated:

$$\frac{M_{k\psi_s}}{M_{k\psi_u}} = \frac{1}{2} \cdot \left(\frac{\sigma \cdot L'_r}{L'_{r\sigma}} + \frac{L'_{r\sigma}}{\sigma \cdot L'_r} \right) \quad (19)$$

Also, since the electromagnetic torque is interpreted as output exergy, based on the observation $\Psi'_r = \Psi_u/\sqrt{2} = ct.$, at $\Psi'_r = ct.$ a relationship for the electromagnetic torque M could be useful within the exergetic analysis:

$$M = M_{k\psi_u} \cdot \frac{L'_{r\sigma}}{R'_r} \cdot \omega_r \quad (20)$$

Graphically, curves of the induction machine electromagnetic torque $M/M_{k\psi_s} = f(\omega_r)$ at $\Psi_s = ct.$, $\Psi_u = ct.$, and $\Psi'_r = ct.$, respectively, are presented in Fig. 11.

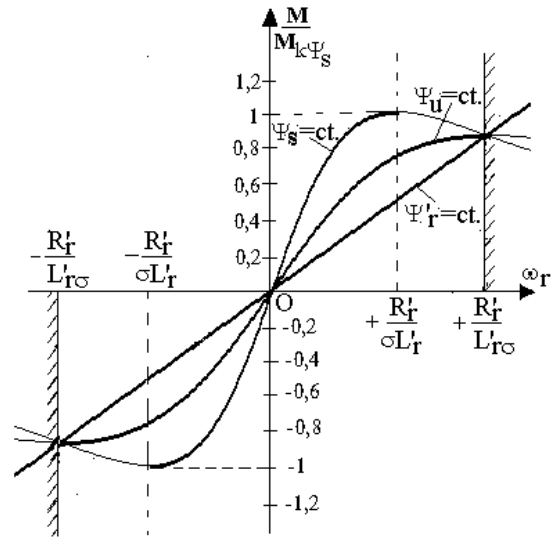


Fig. 11 Curves of $M/M_{k\psi_s} = f(\omega_r)$ at constant flux

3.1.2 Stator Currents Comparison at $\Psi_s = ct.$, $\Psi_u = ct.$ and $\Psi'_r = ct.$

According to relationship (15) for the constant flux levels, the stator current I_s expressions become as follows:

a) When stator flux is constant $\Psi_s = ct.$:

$$I_s = \frac{\psi_s}{L_s} \cdot \sqrt{\frac{1 + \left(\frac{L'_r}{R'_r} \cdot \omega_r\right)^2}{1 + \left(\frac{\sigma \cdot L'_r}{R'_r} \cdot \omega_r\right)^2}} \quad (21)$$

b) When useful flux is constant $\Psi_u = ct.$:

$$I_s = \frac{\psi_s}{L_s} \cdot \frac{\sqrt{2}}{\sqrt{1 + \left(\frac{\sigma \cdot L'_r}{L'_{r\sigma}}\right)^2}} \cdot \sqrt{\frac{1 + \left(\frac{L'_r}{R'_r} \cdot \omega_r\right)^2}{1 + \left(\frac{L'_{r\sigma}}{R'_r} \cdot \omega_r\right)^2}} \quad (22)$$

c) When rotor flux is constant $\Psi'_r = ct.$:

$$I_s = \frac{\psi_s}{L_s} \cdot \frac{1}{\sqrt{1 + \left(\frac{\sigma \cdot L'_r}{L'_{r\sigma}}\right)^2}} \cdot \sqrt{1 + \left(\frac{L'_r}{R'_r} \cdot \omega_r\right)^2} \quad (23)$$

Graphically, Fig. 12 represents the characteristics of stator current I_s at $\Psi_s = ct.$, $\Psi_u = ct.$, and $\Psi'_r = ct.$, respectively.

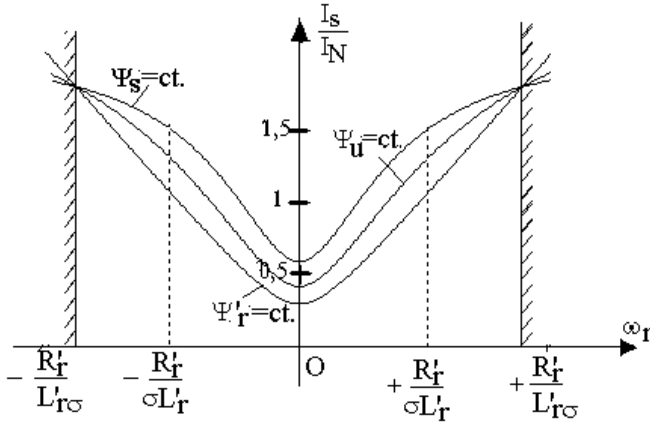


Fig. 12 Characteristics of $I_s/I_N=f(\omega_r)$ at constant flux

3.1.3 Discussion of Torque

The greatest magnitudes of electromagnetic torque are obtained in operating at $\Psi_s=ct.$ Moreover, with the usual approximations $\sigma \cdot L_r'=L_{s\sigma}+L_{r\sigma}$ and $L_{r\sigma} = L_{s\sigma}$, the maximum torque relationship is obtained in the form:

$$M_{k\psi_u} \approx \frac{4}{5} \cdot M_{k\psi_s} \quad (24)$$

This emphasizes that the maximum electromagnetic torque in operating at $\Psi_u = ct.$ is approximately with 20% smaller than the maximum torque in operating at $\Psi_s = ct.$ The ratio of the critical rotor pulsations $\omega_{rk\psi_s}$ and $\omega_{rk\psi_u}$ is:

$$\frac{\omega_{rk\psi_s}}{\omega_{rk\psi_u}} = \frac{L_{r\sigma}}{\sigma \cdot L_r'} \approx \frac{1}{2} \quad (25)$$

This means that an “inferior” maximum torque $M_{k\psi_u}$ is developed at the rotor pulsation with a double value that of the rotor pulsation corresponding to $M_{k\psi_s}$ (or $\omega_{rk\psi_u} = 2 \cdot \omega_{rk\psi_s}$).

Moreover, at the imposed electromagnetic torque, the smallest value of rotor pulsation is obtained in operation with $\Psi_s = ct.$

From Fig. 12 similar conclusions are emphasized with regard to the stator currents. Actually, the smallest values of stator currents I_s are obtained in operation with $\Psi_r' = ct.$

The analysis of induction machine operation with constant flux highlights that only at $\Psi_r' = ct.$ the induction machine mechanical characteristics not have extremum points; they are straight lines. These linear characteristics are preferable for the applications which demand high sustainability dynamics in induction machine operation.

3.2 Modelling of Induction Motor Operating at Variable Frequency and Controlled Flux through Structural Diagram Method

In order to be used with high energy and exergy efficiency in an electrically driven system, modelling is carried out for the induction motor using a structural diagram.

As a complex electromechanical system, the induction motor can be conceptually decomposed into electromagnetic and mechanical subsystems. Between these functional parts, the electromagnetic torque M and the rotor mechanical speed Ω_m interact as internal variables. The induction motor electromagnetic part can be described by the following equations [1,5,7,21-22]:

$$\begin{aligned} \frac{d\underline{\psi}_s}{dt} &= \underline{u}_s - R_s \cdot \underline{i}_s \\ \frac{d\underline{\psi}_{r'}}{dt} &= j \cdot p \cdot \Omega_m \cdot \underline{\psi}_{r'} - R_{r'} \cdot \underline{i}_{r'} \\ \underline{i}_s &= \frac{\underline{\psi}_s - \frac{L_u}{L_r'} \cdot \underline{\psi}_{r'}}{\sigma L_s}; \quad \underline{i}_{r'} = \frac{\underline{\psi}_{r'} - \frac{L_u}{L_s} \cdot \underline{\psi}_s}{\sigma L_{r'}} \\ M &= \frac{3}{2} \cdot p \cdot \text{Im}\{\underline{i}_s \cdot \underline{\psi}_{r'}^*\} \end{aligned} \quad (26)$$

Here, \underline{u}_s denotes the stator voltage vector; \underline{i}_s the stator current vector; $\underline{i}_{r'}$ the rotor current vector; $\underline{\Psi}_s$ the stator flux vector; $\underline{\Psi}_{r'}$ the rotor flux vector; L_u the magnetizing inductance; L_s the stator inductance; $L_{r'}$ the rotor inductance; p the number of pole pairs; R_s the stator resistance; $R_{r'}$ the rotor resistance and $\sigma = 1 - \frac{L_u^2}{L_s \cdot L_{r'}}$ the motor leakage coefficient.

Using equation (26), the structural diagram and the mask block of the induction motor electromagnetic subsystem are depicted in Fig. 13.

The structural diagram of the electromagnetic subsystem can be coupled both with the structural diagram of the machine-side converter through the input variable \underline{u}_s and output variable \underline{i}_s and with the structural diagram of the mechanical subsystem via the input quantity Ω_m and the output quantity M .

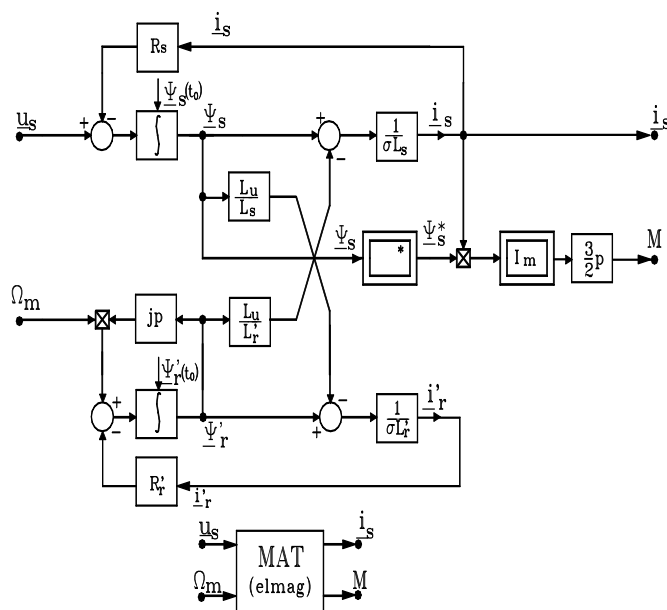


Fig. 13 Structural diagram and mask block for induction machine electromagnetic subsystem

4 Conclusion

The benefits of using sustainability concepts and mathematical modeling to understand the efficiency of electric power equipment which use or convert electrical energy have been demonstrated.

This study demonstrated that modelling the electric power transformer and the induction motor in dynamic regimes according to an industrial ecosystem pattern provided a holistic view of the interactions and symbiosis interrelationships among technical equipment operation and ecological processes.

The main environmental impacts related to the operation phase of a power transformer and an induction motor are caused by the electricity losses of the electric equipment under specific load conditions. The study demonstrates the increase of energy and exergy efficiencies of the induction motor and power transformer in dynamic regimes by implementing sustainability dynamics in mathematical modeling through the structural diagram method.

Through this study we demonstrate that an approach to electric power systems modeling via the structural diagram method can demonstrate, according to the model of an industrial ecosystem, the interactions and the feedback loops among the different variables that describe the three-phase power transformer and induction motor operation.

Directions for future works, as an attempt to reduce or minimize the environmental impacts and

optimize the efficiency of energy use, include advanced modeling and analysis of other electric power equipment dynamic regimes within the framework of industrial ecology.

References:

- [1] Bulucea C.A., Nicola D.A., Rosen M.A., Mastorakis N.E., Bulucea C.A., *Modelling Examples of Sustainable Electric Power Equipment*, Recent Advances in Environmental and Earth Sciences and Economics, Proceedings of the 2015 International Conference on Energy, Environment, Development and Economics (EED 2015) Proceedings of the 2015 International Conference on Geology and Seismology (GESE 2015) Proceedings of the 2015 International Conference on Maritime and Naval Science and Engineering (MANASE 2015) Proceedings of the 2015 International Conference on Water Resources, Hydraulics & Hydrology (WHH 2015), Series: Energy, Environmental and Structural Engineering Series | 38, Zakynthos Island, Greece July 16-20, 2015, pp.108-115.
- [2] Rosen M.A., Bulucea C.A., Using Exergy to Understand and Improve the Efficiency of Electrical power Technologies, *Entropy* 2009, 11, 820-835.
- [3] Nicola D.A., Rosen M.A., Bulucea C.A., Brandusa C., Sustainable Energy Conversion in Electrically Driven Transportation Systems, *Proc. 6th WSEAS Int. Conf. on Engineering Education (EE'09)*, Rhodes, Greece, July 22-24, 2009, pp. 124-132.
- [4] Mastorakis N.E., Bulucea C.A., Nicola D.A., *Modeling of Three-phase Induction Motors in Dynamic Regimes According to an Ecosystem Pattern*, Proc. 13th WSEAS Int. Conf. on Systems (CSCC'09), Rodos (Rhodes) Island, Greece, July 22-24, 2009, pp. 338-346, ISBN: 978-960-474-097-0, ISSN: 1790-2769.
- [5] Nicola D.A., Rosen M.A., Bulucea C.A., Brandusa C., Some Sustainability Aspects of Energy Conversion in Urban Electric Trains, *Sustainability* 2010, 2, 1389-1407.
- [6] United Nations, *The future we want*, United Nations Conference on Sustainable Development, Rio de Janeiro, Brazil, 20-22 June 2012, Available at: http://www.unep.fr/scp/pdf/Rio_The_Future_We_Want.pdf, Accessed on 10 February, 2015.
- [7] Bulucea C.A., Nicola D.A., Mastorakis N.E., Rosen M.A., Understanding Electric Industrial Ecosystems through Exergy", *Recent Researches in Energy & Environment, Proc. of 6th*

- IASME/WSEAS International Conference on Energy & Environment*, University of Cambridge, Cambridge, UK, February 23-25, 2011, pp. 182-191.
- [8] Graedel T.E., On the Concept of Industrial Ecology, *Annual Review of Energy and the Environment*, Vol. 21, November 1996, 69-98.
- [9] Ayres R.U., Industrial Metabolism, In Ausubel J.H., and Sladovich H.E. (eds): *Technology and Environment*, pp. 23-49, National Academy Press, Washington, 1989.
- [10] Graedel T.E., Allenby B.R., *Industrial Ecology*, Prentice Hall, New Jersey, 1995.
- [11] Allenby B.R., *Industrial Ecology: Policy Framework and Implementation*. Prentice-Hall, New Jersey, 1999.
- [12] Allenby B.R., Industrial Ecology, Information and Sustainability, *Foresight: Journal of Future Studies, Strategic Thinking and Policy*, Vol. 2, No. 2, 2000, 163-171.
- [13] Dincer I., Rosen M.A., *Exergy: Energy, Environment and Sustainable Development*, 2d ed., Elsevier: Oxford, UK, 2013.
- [14] Rosen M.A., A Concise Review of Energy-Based Economic Methods, *Proc. 3rd IASME/WSEAS Int. Conf. on Energy & Environment*, Cambridge, UK, Feb. 23-25, 2008, 136-142.
- [15] Wall G., Gong M., On Exergy and Sustainable Development, Part I: Conditions and Concepts, *Exergy: An International Journal*, Vol. 1, No. 3, 2001, 128-145.
- [16] Wall G., Exergy tools, *Proc. Inst. Mechanical Engineers, Part A: J. Power and Energy*, Vol. 217, 2003, 125-136.
- [17] LCA study of current transformers, *DANTES project co-funded by the EU Life-Environment Program*, Available at: http://www.dantes.info/Publications/Publication_doc/DANTES%20ABB%20LCA%20study%20of%20instrument%20transformers.pdf, Accessed on 14 March 2015.
- [18] Nicola D.A., Bulucea C.A., *Electrotechnics, Electrical Equipment and Machines*, Vol. II "Electrical Equipment", SITECH Publishing House, Craiova, 2005.
- [19] Bulucea C.A., Nicola D.A., Mastorakis N.E., Cismaru D.C., *Modelling of Electrical Transformers in Dynamic Regimes*, Recent Advances in Electric Power Systems, High Voltages, Electric Machines, Proc. 9th WSEAS/IASME Int. Conf. on Electric Power Systems, High Voltages, Electric Machines, University of Genova, Genova, Italy, October 17-19, 2009, 188-195.
- [20] Bulucea C.A., Nicola D.A., Mastorakis N.E., Dondon Ph., Bulucea C.A., Cismaru D.C., Fostering the Sustainability of Power Transformers, *Recent Researches in Environmental & Geological Sciences, Proc. of 7th WSEAS International Conference on Energy and Environment (EE'12)*, Kos Island, Greece, July 14-17, 2012, pp. 72-81.
- [21] Nicola D.A., *Electric Traction (Tractiune electrica)*, Universitaria Publishing House, Craiova, Romania, 2012.
- [22] Nicola D.A., Rosen M.A., Bulucea C.A., Cismaru D.C., Some Aspects of Sustainable Energy Conversion in Electric Railway Vehicles with Traction Induction Motors, *Recent Advances in Systems Science: Proc. 17th Int. Conf. on Systems*, Rhodes Island, Greece, July 16-19, 2013, pp. 44-53.
- [23] Chatelain, *Machines électriques (Electrical Machines)*, PPUR, Lausanne, 1989.
- [24] Kaller R., Allenbach J.M., *Traction Electrique (Electrical Traction)*, Vol. 1-2, PPUR, Lausanne, 1995.
- [25] Buhler H., *Reglage de Systemes d'Electronique de Puissance*, Vol. I, PPUR, Lausanne, 1997.
- [26] Potter S., Exploring Approaches Towards a Sustainable Transport System, *International Journal of Sustainable Transportation*, Vol. 1, Issue. 2, 2007, 115-131.
- [27] MacHaris C., Van Mierlo J., Van Den Bossche P., Combining Intermodal Transport with Electric Vehicles: Towards More Sustainable Solutions, *Transportation Planning and Technology*, Vol. 30, Issue 2-3, 2007, 311-323.